Biochimica et Biophysica Acta 1848 (2015) 51–59

Contents lists available at ScienceDirect

Biochimica et Biophysica Acta

journal homepage: www.elsevier.com/locate/bbamem

Mechanosensitive Ca^{2+}-permeable channels in human leukemic cells: Pharmacological and molecular evidence for TRPV2

Igor Pottosin [a], Iván Delgado-Enciso [b], Edgar Bonales-Alatorre [a], María G. Nieto-Pescador [a], Eloy G. Moreno-Galindo [a], Oxana Dobrovinskaya [a,*]

[a] Center for Biomedical Research, University of Colima, Colima, Mexico
[b] School of Medicine, University of Colima, Colima, Mexico

ARTICLE INFO

Article history:
Received 7 May 2014
Received in revised form 12 September 2014
Accepted 15 September 2014
Available online 28 September 2014

Keywords:
T-lymphocyte
Plasma membrane stretch
Mechanosensitive channel
Calcium
TRPV2

ABSTRACT

Mechanosensitive channels are present in almost every living cell, yet the evidence for their functional presence in T lymphocytes is absent. In this study, by means of the patch-clamp technique in attached and inside-out modes, we have characterized cationic channels, rapidly activated by membrane stretch in Jurkat T lymphoblasts. The half-activation was achieved at a negative pressure of ~50 mm Hg. In attached mode, single channel currents displayed an inward rectification and the unitary conductance of ~40 pS at zero command voltage. In excised inside-out patches the rectification was transformed to an outward one. Mechanosensitive channels weakly discriminated between mono- and divalent cations (P_{Ca}/P_{Na} ~ 1) and were equally permeable for Ca^{2+} and Mg^{2+}. Pharmacological analysis showed that the mechanosensitive channels were potently blocked by amiloride (1 mM) and Gd^{3+} (10 μM) in a voltage-dependent manner. They were also almost completely blocked by ruthenium red (1 μM) and SKF 96365 (250 μM), inhibitors of transient receptor potential vanilloid 2 (TRPV2) channels. At the same time, the channels were insensitive to 2-aminoethoxydiphenyl borate (2-APB, 100 μM) or N-(p-amylcinnamoyl)anthranilic acid (ACA, 50 μM), antagonists of transient receptor potential canonical (TRPC) or transient receptor potential melastatin (TRPM) channels, respectively. Human TRPV2 siRNA virtually abolished the stretch-activated current. TRPV2 are channels with multifaceted functions and regulatory mechanisms, with potentially important roles in the lymphocyte Ca^{2+} signaling. Implications of their regulation by mechanical stress are discussed in the context of lymphoid cells functions.

1. Introduction

Living cells respond to a variety of mechanical stimuli, from osmotic stress to local mechanical deformations of the membrane. The sequence of events activated by initial mechanical stimulation and leading to the specific cellular response is the subject of intensive studies in different types of cells. Nowadays, it is well established that the transduction of mechanical stimuli to electrical and, in some cases, also to Ca^{2+} signals is mediated by mechanosensitive channels (MSCs), which are found in all kingdoms, including prokaryotes (for a review see [54,22]). In mammals, three groups of channels were proved to show mechanosensitive properties: degenerins or epithelium Na^+ channels (ENaC), some two-pore domain K^+-selective (K2P) channels, and certain members of the transient receptor potential (TRP) channels family [39]. In addition, recently discovered Piezo channels appear to form non-selective (Ca^{2+} ~ Mg^{2+} ~ Na^+ ~ K^+) rapidly-inactivating mechanosensitive cation channels or be a part of such channel [11,17,48]. TRPs, which were proved to be directly or indirectly gated by mechanical stretch, namely, TRPC 1 and 6, TRPV1, 2 and 4, TRPM3, 4, and 7, TRPP 1 and 2, and TRPA1, form cationic MSC in most cases only weakly discriminating between Na^+ and Ca^{2+} [39].

Very little is known about MSC in lymphoid cells. However, for a variety of physiological processes taking place in lymphocytes, the ability to respond rapidly to mechanical stimulation seems to be crucial. Indeed, circulating lymphocytes are affected by fluid flow, variations in osmolarity and blood pressure. They also change their shape during extravasation and infiltration of tissues. Antigen recognition, lymphocyte maturation and activation are vitally important processes, where cell–cell interactions occur. During direct contacts, cells may undergo mechanical deformation and membrane stretch. For distant indirect interactions, lymphocytes produce and secret the variety of lymphokines. It was shown recently that mechanical stress may provoke lymphokine release [29].

Abbreviations: 2-APB, 2-Aminoethoxydiphenyl borate; ACA, N-(p-amylcinnamoyl) anthranilic acid; K2P channels, Two-pore domain K^+ channels; MSC, Mechanosensitive channel; RR, Ruthenium red; TRP, Transient receptor potential; TRPC, Transient receptor potential canonical; TRPM, Transient receptor potential melastatin; TRPP, Transient receptor potential polycystic; TRPV, Transient receptor potential vanilloid.

* Corresponding author at: Centro Universitario de Investigaciones Biomédicas, Universidad de Colima, Av. 25 de Julio 965, Villa San Sebastian 28045 Colima, Col. Mexico. Tel.: +52 312 3161000x47454; fax: +52 312 3161129.
E-mail address: oxana@ucol.mx (O. Dobrovinskaya).

http://dx.doi.org/10.1016/j.bbamem.2014.09.008
0005-2736/

T-cells are able to regulate their volume under osmotic stress. Swelling can be sensed by volume-sensitive outward-rectifying Cl^- channels, VSOR [36,34] and regulated volume decrease is achieved by parallel operation of Cl^- and K^+ channels, with a potential contribution of Kv1.3, KCa3.1 and different K2P channels [6,4]. Notably, regulated volume decrease is Ca^{2+}-independent in mature T lymphocytes, but in thymocytes and Jurkat lymphoblasts it is regulated by swelling-activated Ca^{2+} influx, which is 100-times less sensitive to Gd^{3+} as compared to a dominant lymphocyte Ca^{2+}-influx channel, CRAC [53]. Potentially, volume decrease can be mediated by some Ca^{2+}-permeable channels from the TRP family. In T-cells, the expression of different TRPC (1, 3, 6), TRPM (2, 4, 7), and TRPV (1, 2) were detected. TRPC6 was not detected in Jurkat; instead, the expression of TRPC4, TRPC5, and TRPV6, which are rarely present in T-cells from healthy donors, was reported [67]. Of them, only functional roles of TRPM (4, 7 and to a less extent, 2) were revealed for T-cells (for a review see [6,15]). TRPM4 is unique channel with a very low Ca^{2+} permeability, so it cannot be involved in the stretch-activated Ca^{2+} influx. Yet, multiple TRP family members still left, which potentially encode MSC in T-cells and lymphoblasts. This study was undertaken to check for the presence of the TRP-like MSCs in Jurkat cells and to verify their identity on the basis of ionic selectivity and conductance, pharmacological profile and, eventually, by means of small interfering RNA.

2. Materials and methods

2.1. Cell preparation and culture condition

Jurkat cells (clone E6-1) were kindly provided by Dr. Yvonne Rosenstein (Instituto de Biotecnología, UNAM, México). Cells were cultured in Advanced RPMI 1640 medium supplemented with 5% heat-inactivated fetal calf serum, 100 U/ml penicillin, 100 μg/ml streptomycin, and 1% of GlutaMAX™ (all from Invitrogene, Carlsbad, CA, USA) at 37 °C in a humidified atmosphere (5% CO_2, 95% air). Cells were maintained in the logarithmic growth phase by daily medium refreshment.

2.2. TRPV2 silencing by small interfering RNA (siRNA)

siRNA transfection experiments were carried out using as a starting point the Supplementary Protocol for Jurkat cells provided by Quiagen. The protocol was optimized for our conditions to achieve both maximal cell survival and transfection efficiency. Resulting protocol was as follows: 1×10^6 cells in 250 μl of Advanced RPMI 1640 medium without serum and antibiotics were transfected with 1.75 μl of Lipofectamine 2000 transfection reagent (Life Technologies) and 1250 ng of fluorescein-coupled small interfering RNA (siRNA) against TRPV2 (FlexiTube siRNA S102781359 from Quiagen), the concentration value being inside the range for cationic lipids mediated siRNA transfection in Jurkat cells recommended by Quiagen (140–562 ng/100 μl). siRNA sequences were: sense strand 5′-GAGGAUCUUUCCAACCACATT-3′, antisense strand 5′-UGUGGUUGGAAAGAUCCUCTG-3′. Additionally, a negative siRNA-control with scrambled sequence (siRNA 1027310 from Quiagen) was used to transfect cells in the same conditions. After 5 h incubation at 37 °C in a humidified atmosphere (5% CO_2, 95% air), the medium with transfection complexes was replaced for 250 μl Advanced RPMI 1640 medium supplemented with 2.5% heat-inactivated fetal calf serum, 100 U/ml penicillin, 100 μg/ml streptomycin, and 1% of GlutaMAX™ (all from Invitrogen). The cells were allowed to recover during at least 1 h, and the effect of silencing was tested by patch-clamp in cell-attached configuration and qRT-PCR during the next 6 h. Cell survival was estimated by trypan blue exclusion test. Transfection efficiency was analyzed and the images were obtained by confocal microscopy using an LSM 700 system (Carl Zeiss) coupled to an inverted Observer.Z1 microscope, equipped with 40× oil-immersion objectives, 488 nm laser, and ZEN imaging software. The settings were: laser power 2%, pinhole $\Phi = 1.00$ AU; detector gain = 685; line step: 1; scan speed: 6; data depth: 16 bit; mode: line; method: mean; scan number: 2; zoom: 1.

2.3. Electrophysiology

Patch-clamp experiments were performed in attached and inside-out configurations using an Axopatch 200A Integrating Patch-clamp amplifier (Axon Instruments). Patch pipettes were pulled from Kwik-Fil 1B150F-4 capillaries (World Precision Instruments, Sarasota, FL, USA) and fire-polished. Patch electrodes were filled with a solution containing (in mM): 134 KCl, 2 $MgCl_2$, 1 $CaCl_2$, 10 EGTA, 10 HEPES–KOH (pH 7.4). The resistance of patch electrodes filled with this solution was 3–5 MΩ. For cell-attached recordings, bath solution ("160 NaCl") contained (in mM): 150 NaCl, 5 KCl, 1 $MgCl_2$, 2.5 $CaCl_2$, and 10 HEPES–NaOH (pH 7.4). For ion selectivity measurements in the inside-out configuration, different bath solutions were implemented. One was identical to the bath solution described above or 10 times diluted, "16 NaCl." K^+ to Cl^- selectivity was evaluated with a bath, containing (in mM): 9 KCl, 10 HEPES–KOH (pH 7.4). For Na^+/Ca^{2+} or Na^+/Mg^{2+} selectivity measurements, bath solution was the same as for cell-attached measurements ("160 NaCl"), whereas pipette solution contained (in mM): 50 $CaCl_2$ or $MgCl_2$, 5 HEPES–$Ca(OH)_2$ (pH 7.4). Osmolality of all solutions was adjusted to 310 mOsm. For mechanical patch stimulation, a constant negative pressure to the patch pipette interior was applied manually and its magnitude was verified with a portative manometer. Records were low-pass filtered at 5 kHz, digitized using a DigiData 1200 Interface (Axon Instruments, Foster City, CA), transferred to a personal computer and analyzed using the pClamp 6.0 software package (Axon Instruments, Foster City, CA).

In TRPV2 silencing experiments, epifluorescence was used to distinguish siRNA transfected (fluorescein-positive) and non-transfected cells. To prove the effect of TRPV2 silencing on stretch-activated current, electrophysiological records were performed on membrane patches from siRNA positive and negative cells, assayed in a random order. Three independent transfection experiments were realized. Simultaneously, knockdown efficiency was determined by single cells qRT-PCR analysis. Single cells were recollected by aspiration during patch-clamp experiments, using glass micropipettes with a tip opening ca. 20 μm fabricated on the P-97 Flaming/Brown Micropipette Puller (Sutter Instruments, Novato, CA, USA).

2.4. Single-cell qRT-PCR

Cells were submitted to single-cell one-step real-time duplex RT-PCR analyses using Roche Light Cycler version 1.5. The QuantiFast Probe assay RT-PCR Plus Kit for dual detection of TRPV2 and GAPDH (Quiagen) was used. Corresponding QuantiFast Probes labeled with different fluorochromes were: TRPV2/FAM (Cat. No QF00207102) and GAPDH/MAX (Cat No QF00531132). Experimental procedures followed the manufacturer's protocol. Cells were emptied directly into the one-step qRT-PCR reaction, without RNA purification. Before the initiation of the cDNA synthesis, samples were incubated at 80 °C over 5 min as described elsewhere [3]. Cells transfected with siRNA against TRPV2, non-transfected cells, and siRNA negative controls (cells, transfected with siRNA 1027310 from Quiagen) were assayed. To determine relative expression of the mRNAs, real-time RT-PCR data were analyzed by the comparative $\Delta\Delta C_T$ method as previously described [58].

2.5. Data analysis

Data are reported as mean ± SEM. Where appropriate paired or unpaired Student's *t* test was used to evaluate statistical difference. A two-tailed probability value of less than 0.05 ($p < 0.05$) was considered statistically significant.

3. Results

3.1. Membrane stretch activates Ca^{2+}-permeable cation channels in Jurkat cells

Jurkat cells easily form high resistance seals (10–40 GΩ) with a patch pipette after application of light suction (see an example in Fig. 1b, where the leak resistance was 17 GΩ). Attached patches, inspected immediately after gigaseal formation often show some residual channels' activity, which normally ceased after 1–2 min. Then, ramp wave protocols were applied in a following sequence: three 1 s-episodes without suction, further three ramps under negative pressure (60 mm Hg), followed by four ramps at zero pressure. Alternatively, negative pressure was applied for few seconds at a fixed voltage. Mechanical stimulation caused a rapid activation of several mechanosensitive channels (MSCs) in up to 80% of inspected patches (Fig. 1a, b). Their activity did not show a significant inactivation within few seconds of stimulation, yet after turning off the suction, channels' activity displayed a relatively slow deactivation (Fig. 1a). Deactivation of the MSC activity was much faster (<1 s) while running a sequence of voltage ramps. Thus, before and after application of the suction normally only leak currents were recorded (Fig. 1b). After subtraction of leak currents and normalization of resulting I/V curves by dividing them through a number of visible channels, single channel I/V relations were obtained (Fig. 1c). As can be seen from the figure, single channel currents reversed at potentials close to the resting membrane voltage (zero command voltage) and displayed a notable inward rectification. Stable activity of MSCs can be repeatedly reproduced over at least 15 min in cell-attached configuration without a notable rundown. Yet, patch excision resulted in a faster rundown, especially in the presence of high (millimolar) divalent cation concentrations at either membrane side. We were unable to induce MSC activity in outside-out patches. Therefore, to assay the dose–response dependence of the MSC activity and effects of external drugs we have used exclusively the cell attached configuration, whereas for the single channel ion selectivity measurements we have used inside-out patches. The latter allowed control of ionic conditions at both membrane sides.

To reveal mechanosensitivity, we have applied variable negative pressure to the patch-pipette interior at fixed potential of −50 mV (Fig. 2). As can be seen, MSC activity could be detected at pressure as low as 20 mm Hg, and saturated at negative pressures >80 mm Hg by absolute value, with a midpoint around 50 mm Hg.

MSC in Jurkat cells revealed a high degree of the K^+/Cl^- selectivity as evidenced by the data in Fig. 3b. It has also a comparable permeability for K^+ and Na^+ (Fig. 3a) or for Na^+ and Ca^{2+} or Mg^{2+} (Fig. 3c). Interestingly, in inside-out configuration, single MSC current–voltage relations displayed an outward rectification (Fig. 2a, b), compared to the inward rectification in on-cell patches (Fig. 1c).

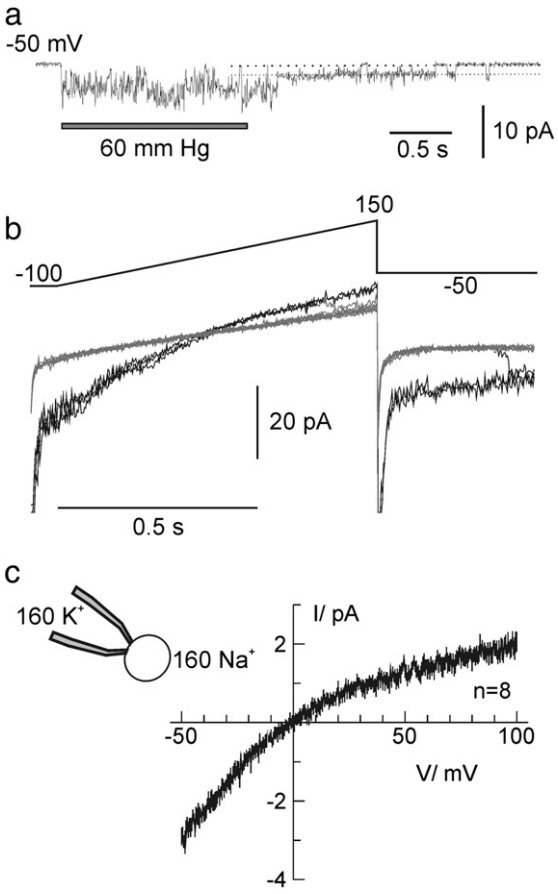

Fig. 1. Membrane stretch evokes activation of ion channels in cell-attached patches. **a.** Examples of an on-cell recording of the activity of mechanosensitive channels in Jurkat cells. After obtaining a tight seal with cell membrane, command voltage was clamped to −50 mV (cytosol minus exterior) and application of a suction pulse (60 mm Hg) as indicated resulted in the rapid and reversible opening of several mechanosensitive channels. **b.** Response to a ramp-wave voltage protocol (shown in the inset); first three ramps were applied without suction (no channel activity), followed by three ramps under application of negative pressure of 60 mm Hg, and further four ramps with a pressure released (cessation of the channel activity). Gray traces are leak currents (with zero channel activity). **c.** To obtain unitary current–voltage (I/V) relationships for mechanosensitive channels, ramps with channel activity were used and averaged leak current was subtracted; resulting I/V curves were further divided by a number of open channels, using resolved single channel records, as one in **a** for a proper scaling. Data are presented as mean ± SE, data for eight individual Jurkat cells were averaged.

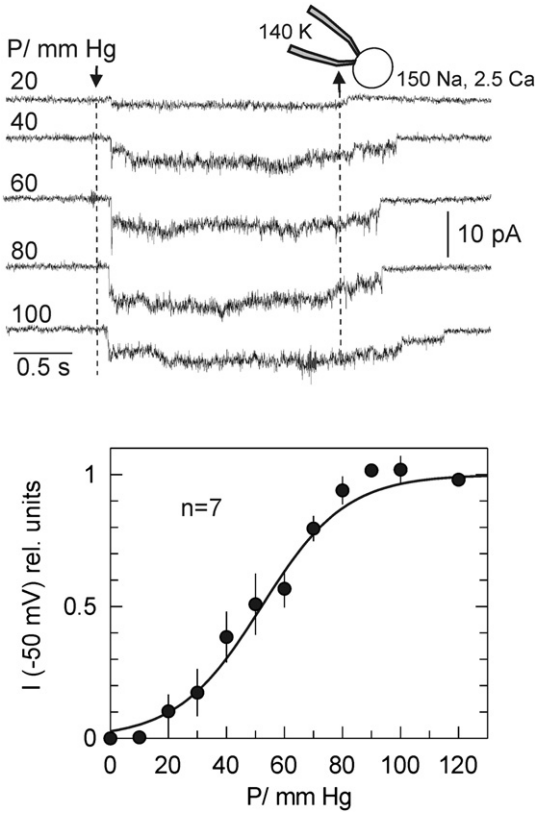

Fig. 2. Evaluation of the mechanosensitivity of stretch-activated channels in Jurkat cells. Example of channels' activation at fixed voltage (−50 mV) in response to increasingly higher negative pressure, applied and relieved as indicated by arrows. Normalized channel activity as a function of applied pressure, responses were normalized to that at 100 mm Hg; data for seven individual cells were averaged and presented as means ± SE. Fitting yielded a midpoint for the response at the pressure of 52 ± 2 mm Hg.

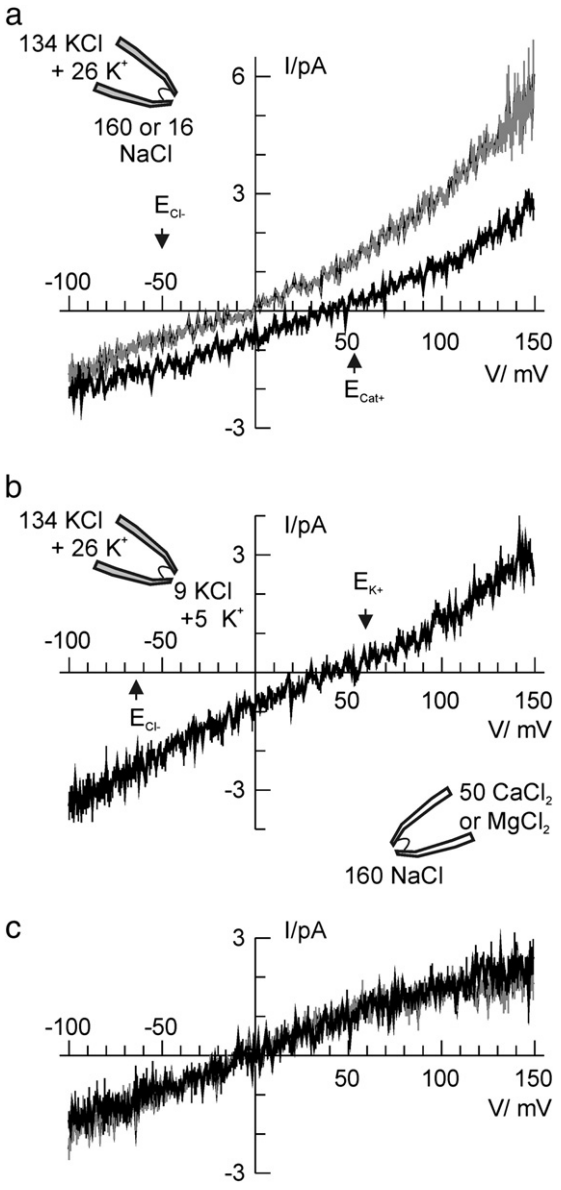

Fig. 3. Selectivity of the mechanosensitive channels in Jurkat cells. All measurements were done on isolated inside-out patches; channel-mediated current was evaluated by applying voltage-ramp protocol as described in Fig. 1b, c. **a, b.** Stretch-activated channels were selective for cations against Cl^- but did not differentiate between K^+ and Na^+. Cationic selectivity is evidence by a positive shift of reversal potential upon a 10-fold dilution of the bath; mind the opposite shift of equilibrium potential for Cl^-. On the other hand, zero reversal potential at bi-ionic conditions, KCl against approximately the same concentration of NaCl (gray curve) implied equal permeability for K^+ and Na^+. In **b**, reversal potential of the single channel current approached E_{K+} and is far from E_{Cl-}, implying a high K^+/Cl^- selectivity. **c.** Stretch activated channels do not differentiate between Na^+ (160 mM in the bath) and divalent cations (50 mM of $CaCl_2$, black curve, or $MgCl_2$, gray curve, in the bath). For each trace, unitary I/V curves from five to nine individual cells were averaged.

3.2. Pharmacological profile of stretch-activated channels

In continuation, we performed the pharmacological analysis of the MSC in Jurkat cells. To do this, we have introduced a blocker into the patch-pipette (in case of Gd^{3+} and ruthenium red (RR), EGTA and divalent cations were excluded from the standard pipette solution). To make a comparison with a control feasible and to minimize a difference, caused by a variation of channels' expression in different cells, we took an advantage of a relatively large size of lymphoblasts, so that each cell could be patched twice (up to five times), with different patch-pipettes containing or not the blocker of interest. When multiple patching was not possible with the same cell for any reason (e.g. cell disruption), these results were discarded. The first two blockers used were amiloride, a non-specific blocker of epithelium Na^+ channels and antiporters, as well as of some MSC and TRP channels (see [33,12] and the references therein), and Gd^{3+}, a blocker of a variety of non-selective cation channels. Both drugs blocked the MSC mediated current in a voltage-dependent manner, with a much more pronounced effect on the current at negative membrane potentials (Fig. 4a, b). As both blockers are positively charged, this implied that their binding site lies well within a voltage drop across the membrane. Moreover, blockage at negative potentials was not complete as evidenced by small, but significant offset of the relative current (Fig. 4b). This observation suggests that both cations may be forced to pass across the whole MSC pore at large negative potentials.

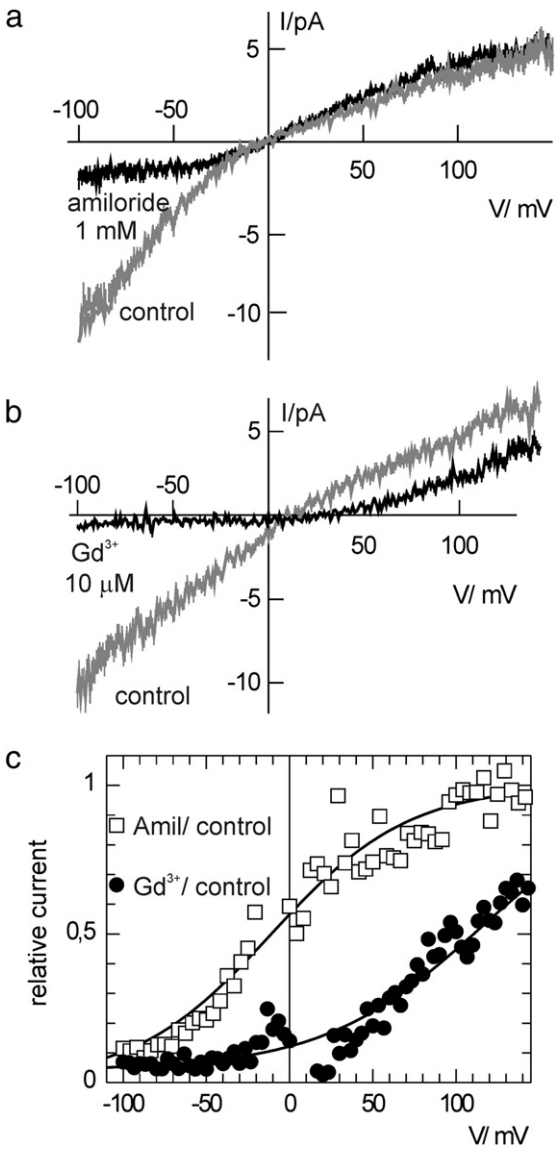

Fig. 4. Voltage dependent block of the stretch-activated channels by amiloride and Gd^{3+}. In **a, b** control and test measurements were made by patching the same cell with a pair of pipettes, with or without the drug. I/V curves obtained from a single cell normally reflected multiple mechanosensitive channels openings in a cell-attached patch; five separate cells were averaged for **a,** and nine for **b. c.** Relative currents, in the presence of drug to that in control, as a function of membrane voltage, were fitted with a modified Boltzmann relation, yielding mean voltage sensitivity ($z\delta$) value of 0.64 and 0.52 for amiloride and Gd^{3+}, respectively. Mind a small but significant offset of the relative current at large negative voltages.

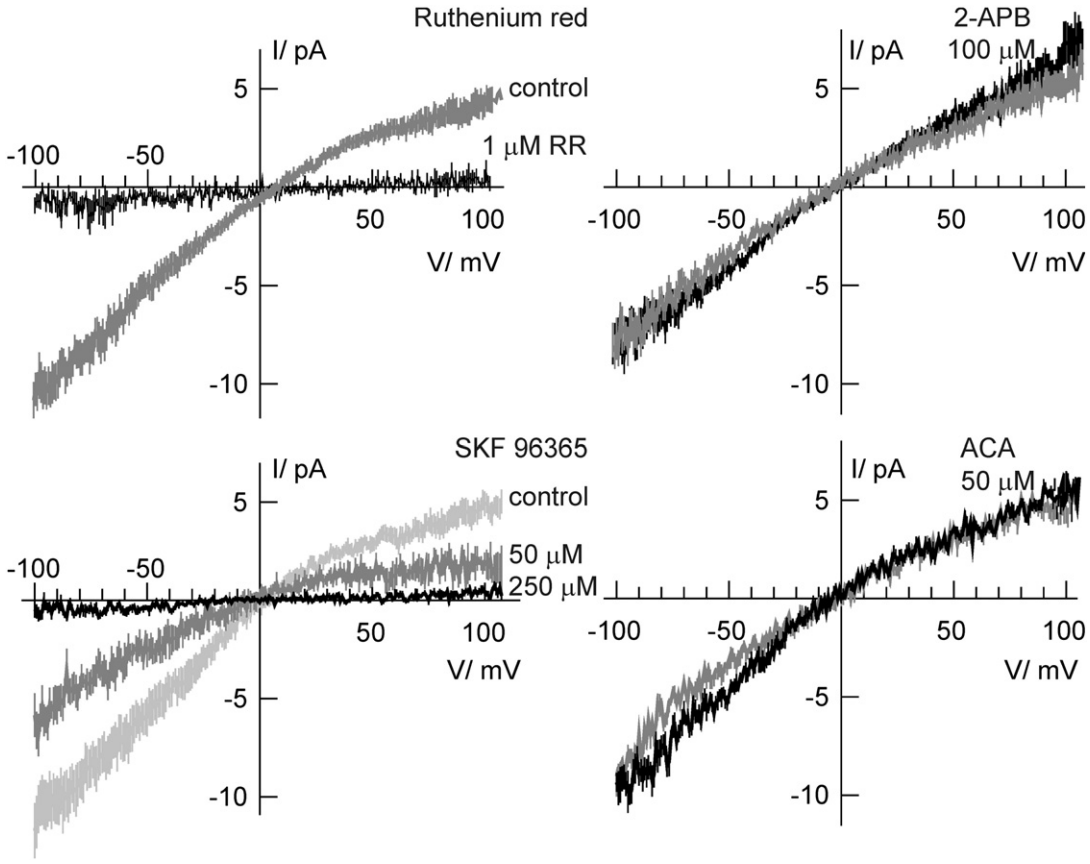

Fig. 5. Pharmacological analysis of the channel-mediated mechanosensitive currents in Jurkat cells. Ramp-wave protocols were applied, and currents were evoked by 60 mm Hg negative pressure and subtracted by leak currents, measured before and after the pressure application. All measurements were performed on cell-attached patches, each control and test measurement was done by patching a single cell with a pair of pipettes, without and with indicated concentration of the drug, and so repeated for each drug on five to six cells, data are means ± SE.

Data in Fig. 5 evidenced that MSC in Jurkat cells were almost completely blocked by RR (1 μM), inhibitor of different Ca^{2+}-permeable channels (including all members of TRPV family) and transporters, and also by SKF 96365, blocker of store- and receptor operated Ca^{2+} entry as well as of some TRP channels [65,19,21]. At the same time, 2-aminoethoxydiphenyl borate (2-APB), initially used as a blocker of inositol 1,4,5-trisphosphate receptor and store-operated Ca^{2+} entry, which also blocks all members of TRPC and TRPM subfamilies (see [19]; and the references therein) was completely inefficient (Fig. 4). N-(p-amylcinnamoyl)anthranilic acid (ACA), inhibitor of phospholipase A2, which directly blocks a variety of TRP channels [20] was also inefficient.

Taken together, the pharmacological profile of the channel of interest better matches the characteristics of the TRPV2 channel (see Discussion for more details). Considering also that in human lymphocytes TRPV2 is the most abundantly expressed among TRPV family members [60], the effect of TRPV2 silencing on stretch-activated current was evaluated in the subsequent set of experiments.

3.3. TRPV2 silencing with siRNA virtually abolished stretch-activated current

Jurkat belong to "hard-to-transfect" cells. In our hands, the efficiency of siRNA transfection achieved 20–30% (Fig. 6a) without affecting cell survival (98–100%). Patch-clamp and single cell qRT-PCR experiments were performed between 6 and 12 h after the start of transfection. In non-transfected cells, the occurrence of mechanosensitive current was detected in 82% of cells (as compared to 80–90% routinely observed for Jurkat cells in the logarithmic growth phase), whereas only 18% of cells with a visible green fluorescence displayed a detectable current in attached patches in response to suction. TRPV2 mRNA expression and stretch-activated current were strongly inhibited in TRPV2 siRNA transfected cells (Fig. 6b, c).

4. Discussion

Jurkat cells, the experimental model of the present study, show some differences in ion channel expression, when compared to healthy mature T cells [6]. Considering that leukemic cell lines are derived from different subsets of immature T cells where additional genetic lesions occurred [64], these differences may reflect both maturation and leukemogenesis processes. However, stretch-activated channels have been shown to be present ubiquitously in mammalian cells [54,22]. Although healthy lymphocytes and leukemic cells are exposed to mechanical stimuli constantly during the performance of their physiological functions, electrophysiological studies of stretch-activated channels on this type of cell are scarce [61]. To the best of our knowledge, the question concerning with the presence of mechanically gated ion channels in lymphoid T cells has never been addressed. At the same time, quantitative RT-PCR technique revealed the expression of several members of the three potentially mechanosensitive subfamilies TRPC, TRPV and TRPM in human lymphocytes and Jurkat cells [67]. It should be noted that only for a couple of TRP channels relatively selective agonists or blockers are available, so that the channel identifying strategy in the case of this family cannot be based on the usage of single specific drugs. Rather, a variety of nonspecific blockers, like RR, binding to the most of Ca^{2+}-binding sites (e.g. of calmodulin or those within a large variety of Ca^{2+} and Ca^{2+}-permeable channels and transporters) or 2-

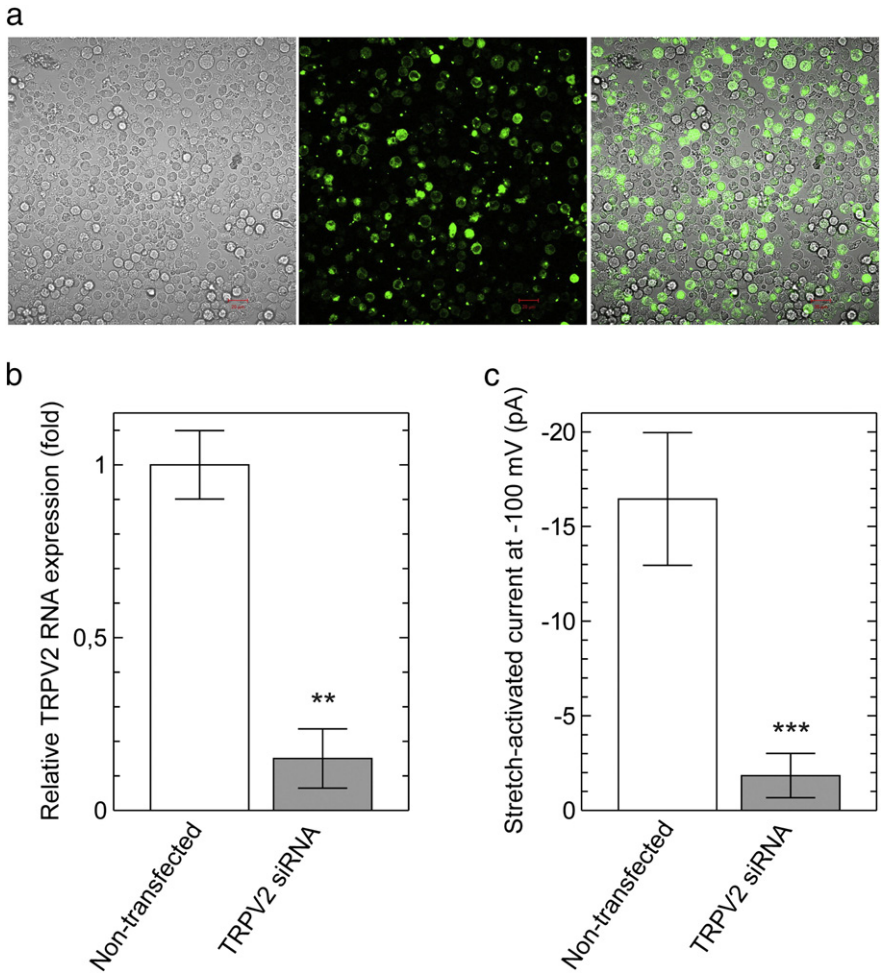

Fig. 6. Effect of TRPV2 siRNA transfection on TRPV2 mRNA expression and stretch-activated current in Jurkat cells. **a.** Visualization of efficiency in TRPV2 siRNA uptake by Jurkat cells in culture. The images of living cells are obtained after 5 h of incubation with fluorescein-labeled TRPV2 siRNA. Brightly fluorescent green cells internalized the siRNA. Phase contrast (left), fluoresceine (middle) and merged (right) images are presented. Scale bar: 20 μM. **b.** Relative expression of TRPV2 mRNA normalized to GAPDH mRNA expression. TRPV2 siRNA transfected ($n = 3$) and non- transfected ($n = 3$) cells were analyzed by single cell real-time qRT-PCR. Data are means ± SE; $^{**}p < 0.005$. **c.** Amplitude of the stretch-activated current in cell-attached patches was evaluated at −100 mV in TRPV2 siRNA transfected ($n = 22$) and non-transfected ($n = 23$) cells. Transfected and non-transfected cells present in each of three independent preparations were assayed in a random order. Data are means ± SE; $^{***}p < 0.001$. In **b** and **c**, negative siRNA controls were comparable to non-transfected cells (data not shown).

APB, which is primarily used to inhibit the store-operated Ca^{2+} entry, or lantanides, generic blockers of non-selective cation channels, are used instead [68]. Taken the advantage of existing differences in pharmacological profiles between diverse TRP channels, e.g. lantanides ions instead of block activate selected TRPs or 2-APB inhibit all channels in the TRPC family, but act as an agonist for some TRPV channels, and combining results of such analysis with available selectivity and current-voltage relationship patterns for TRPs, a plausible identification strategy can be

Table 1
Comparative pharmacology of TRP channels reported for Jurkat cells and MSC described in Jurkat cells in the present work.

	Gd^{3+} (La^{3+})	2-APB	ACA	Ruthenium red (RR)	SKF 96365	Permeability		References
						Ca^{2+}/Na^{+}	Mg^{2+}	
TRPC1	+	+	ND	±	+?	~1	ND	[63,73]
TRPC3	+	+	ND	±	+	1.6	+?	[63,75]
TRPC6	+	+	+	ND	+	5	+?	[26,32,70]
TRPM2	−	+?	+	ND	+	0.5–1.6	+	[21,32,50,69,70]
TRPM4	ND	ND	ND	−	ND	<0.05	ND	[72]
TRPM7	±	+	ND	ND	ND*	3	+	[9,31,41]
TRPV1	−**	***	±	+	ND	4 (heat) 10 (vaniloids)	+	[8,20]
TRPV2	+**	−***	ND	+	+	1–3	+	[8,28,25,30,74]
Jurkat MSC	+	−	−	+	+	~1	+	This study

* Inhibited by ACA derivative, flufenamic acid [31].
** Potentiates TRPV1 but inhibits TRPV2 [35].
*** Activates murine TRPV1 and 2 at >100 μM concentration [25]; human TRPV2 shows little or no sensitivity to 2-APB [28,47].

developed. We have collected the published information on the selectivity and pharmacological profile of TRPC, TRPV and TRPM channels obtained on different experimental models, and then compared with our data for the MSC in Jurkat lymphoblasts (Table 1).

Members of the TRPM family can be definitely excluded from possible candidates, due to their preference for monovalent (Na^+) against divalent (Ca^{2+}) cations and to their sensitivity to ACA. TRPCs are inhibited by 2-APB, but Jurkat MSCs were not (Fig. 5). Murine TRPV1–3 are stimulated by 2-APB, but human TRPV2 is hardly affected by this compound [28,47]. Among TRPVs, TRPV1 is potentiated by Gd^{3+} and can be therefore discarded [35]. TRPV4 and TRPV6, display a relatively high and very high Ca^{2+}/Na^+ selectivity ratio, respectively [10,13]. Moreover, TRPV4 mRNA is hardly detected in Jurkat cells [67]. However, gross properties of the TRPV4 channels like I/V rectification, sensitivity to RR, lantanides, and SKF96365 [66,49,24] are reminiscent of properties of the Jurkat MSC reported here, so TRPV4 cannot be fully discarded. The best fit so far, however, was the hTRPV2 channel, which complies with all observed properties of the Jurkat MSC (Table 1; see also the additional argumentation below). For the sake of completeness, it should be noted that there are other TRP subfamilies, whose presence has not been detected in leukocytes so far. But TRPPs possess a relatively high selectivity for Ca^{2+} over Na^+ and display inward rectification [51], which disqualifies them as a molecular correlate for the MSC in Jurkat. On the other hand, TRPA1 does not discriminate between Na^+ and Ca^{2+} and displays a similar rectification to that shown in Fig. 3 [68,51]. It is similarly affected by Gd^{3+}, amiloride, and RR and is mechanosensitive, mediating the sensation of hearing and touch [46,5]. Yet, at zero external Ca^{2+}, single channel conductance of TRPA1 is about 100 pS [46] or several times higher than that for the MSC in Jurkat cells (Fig. 3a).

In human leukocytes, relative expression of the TRPV2 is more than by one order of magnitude higher as compared to TRPV1, 3 and 4 [60]. Diagram of human TRPV2 gene expression pattern was created [56] based on previously undertaken transcriptome analysis [62], where a peculiar expression of TRPV2 in some types of the cells of immune system was demonstrated. TRPV2 mRNA decreased in the sequence: $CD56^-$ NK cells > $BDCA4^+$ dendritic cells > B-lymphoblasts and $CD8^+$ cytotoxic T cells > $CD4^+$ helper T cells, $CD14^+$ monocytes, $CD33^+$myeloid cells > $CD19^+$ B cells > $CD34^+$ hematopoietic stem cells. Several leukemic/lymphoma cell lines were tested as well and all have shown a relatively high level of TRPV2 expression: Raji (Burkitt's lymphoma) > K562 (chronic myelogenous leukemia) > HL60 (promyelocytic leukemia) > Daudi (Burkitt's lymphoma) > MOLT4 (lymphoblastic leukemia). Among all cell types revealed as TRPV2-positive in this study, patch clamp experiments were reported only on K562 cells, where non-selective Ca^{2+}-permeable MSC with a conductance about 20 pS was reported [61]. Unfortunately, no attempts were done to characterize their sensitivity to drugs or pressure-dependence.

Our study is the first report demonstrating the presence of cationic Ca^{2+}-permeable channels gated by plasma membrane deformation/stretch in the Jurkat cell line. Detailed pharmacological analysis demonstrates that, with a great likelihood, these channels are formed by TRPV2. This conclusion was strengthened by the fact that in TRPV2 silenced Jurkat cells membrane stretch did not activate mechanosensitive current in a vast majority of cells. Taking into the account the importance of mechanical stimuli both for healthy and leukemic T cells, findings of the present study put forward further comparative research of the mechanosensitivity in normal and leukemic lymphoid cells.

TRPV2 is a non-selective cation channel with Ca^{2+} permeability [8]. Therefore deformation and stretch of the lymphocyte plasma membrane during migration, cell–cell interaction events or cytokines secretion may result in its activation and contribute to the intracellular Ca^{2+} signaling. In the recent review on the possible role of TRPV2 channels in immune system [56], the patent application by Sauer and Jegla [57] is cited, where silencing of the TRPV2 with shDNA in Jurkat cells impaired T-cell receptor and CRAC-mediated Ca^{2+} signaling. These data suggest TRPV2 as a feasible drug target for immunosuppression. TRPV2 also plays critical role in the binding of particles and phagocytosis by macrophages [38].

TRPV2 channels may be localized in endosomes, controlling Ca^{2+}-release, fusion, and endocytosis [55] and, when activated, translocated to the plasma membrane [23]. Ca^{2+} influx through stretch-activated TRPV2 caused the degranulation in mast cells; these MSCs have a similar dependence on applied pressure as the MSC in this study (Fig. 2) and were sensitive to SKF96365 and RR [74]. Stretch activation of the TRPV2 was demonstrated also in aortic myocytes and alveolar cells [43,16] and in neurons, thus, controlling the axon outgrowth [59]. Pharmacology of TRPVs is extensively reviewed [65], but no specific blocker/antagonist for TRPV2 has been reported so far. In addition to data of Table 1, TRPV2 was reported to be sensitive to amiloride [65]. The pattern, reported here (Fig. 4a, c), i.e. affinity and voltage-dependence, was completely identical to that for intrinsic MSC in oocytes of *Xenopus* (Fig. 7A in [33]). Within TRP channels, amiloride was inefficient with TRPC1 channels, but blocked, albeit in a voltage-independent manner, different TRPP channels [12,1]. Also, TRPA1 block by amiloride showed a very similar voltage-dependence to that reported here [2]. In respect to the voltage-dependence of Gd^{3+} block (Fig. 4b, c) we found a very similar pattern in case of the TRPM-like MIC [18]. A permeable voltage-dependent block by Gd^{3+} and La^{3+} was reported for TRPM7, but this blockage required a high, millimolar instead of micromolar, concentrations of lantanides [41]. Sensitivity of the inward current through the Jurkat MSC to Gd^{3+} coincides with that for the swelling-induced Ca^{2+} influx (SWAC) in immature T-cells [53].

Altered expression or abnormal activity of TRPV2 channel was shown to be associated with cancer, but its precise role in carcinogenesis is still poorly understood. TRPV2 seems to be involved in different processes which may promote tumor progression, but further studies are required to determine its ability as a drug target or prognostic factor in each particular type of malignances. TRPV2 overexpression was evidenced in patients with multiple myeloma [14]. In hepatocellular carcinoma, it was rather associated with medium and well differentiated than poorly differentiated tumors, where it was proposed as a prognostic marker [37]. In prostate cancer, TRPV2 was shown to be involved in cancer cell migration and invasion, and may be specifically implicated in the progression to more aggressive phenotype [40]. Changes in profiling namely increase in expression of full-length, when compared to short splice-variant of TRPV2, were detected in progression toward high-degree urothelial carcinoma [7]. On the other hand, TRPV2 was shown to negatively control proliferation and resistance to Fas-induced apoptosis of glioblastoma multiforme [44]. Although there is a lack of selective pharmacological tools for TRPV2, cannabidiol, the major non-psychotropic cannabinoid compound derived from plant *Cannabis sativa* [27], is a relatively selective TRPV2 agonist [52]. Whereas administration of cannabidiol was shown to induce apoptosis in human T24 bladder cancer cells due to continuous influx of Ca^{2+} through TRPV2, authors proposed it as a potential therapeutic target for human urothelial carcinoma [71]. Some malignances, including glioblastoma and multiple myeloma [45,42], are effectively sensitized to cytotoxic chemotherapeutic agents by triggering of the TRPV2 channels. Bearing in mind the predominant expression of TRPV2 in lymphocytes as compared to the rest of the blood and to the smooth muscle, whereas its expression in other tissues is very low [56], revelation of important functions of this channel in lymphocyte physiology and leukemogenesis is anticipated.

Acknowledgments

Financial support by CONACyT, grants 12897 to OD and 220793 to IP and FRABA (Universidad de Colima), grant 788/12 to IP is gratefully acknowledged. We are thankful for Julio Cesar Villalvazo Guerrero for his help in initial experiments.

References

[1] C. Bai, A. Giamarchi, L. Rodat-Despoix, F. Padilla, T. Downs, L. Tsiokas, P. Delmas, Formation of a new receptor-operated channel by heteromeric assembly of TRPP2 and TRPC1 subunits, EMBO Rep. 9 (2008) 472–479.

[2] T.G. Banke, The dilated TRPA1 channel pore state is blocked by amiloride and analogues, Brain Res. 1381 (2011) 21–30.

[3] M1. Bengtsson, A. Stahlberg, P. Rorsman, M. Kubista, Gene expression profiling in single cells from the pancreatic islets of Langerhans reveals lognormal distribution of mRNA levels, Genome Res. 15 (2005) 1388–1392.

[4] N. Bobak, S. Bittner, J. Andronic, S. Hartmann, F. Mühlpfordt, T. Schneider-Hohendorf, K. Wolf, C. Schmelter, K. Göbel, P. Meuth, H. Zimmermann, F. Döring, E. Wischmeyer, T. Budde, H. Wiendl, S.G. Meuth, V.L. Sukhorukov, Volume regulation of murine T lymphocytes relies on voltage-dependent and two-pore domain potassium channels, Biochim. Biophys. Acta 1808 (2011) 2036–2044.

[5] S.M. Brierley, J. Castro, A.M. Harrington, P.A. Hughes, A.J. Page, G.Y. Rychkov, L.A. Blackshaw, TRPA1 contributes to specific mechanically activated currents and sensory neuron mechanical hypersensitivity, J. Physiol. Lond. 589 (2011) 3575–3593.

[6] M.D. Cahalan, K.G. Chandy, The functional network of ion channels in T lymphocytes, Immunol. Rev. 231 (2009) 59–87.

[7] S. Caprodossi, R. Lucciarini, C. Amantini, M. Nabissi, G. Canesin, P. Ballarini, A. Di Spilimbergo, M.A. Cardarelli, L. Servi, G. Mammana, G. Santoni, Transient receptor potential vanilloid type 2 (TRPV2) expression in normal urothelium and in urothelial carcinoma of human bladder: correlation with the pathologic stage, Eur. Urol. 54 (2008) 612–620.

[8] M.J. Caterina, T.A. Rosen, M. Tominaga, A.J. Brake, D. Julius, A capsaicin-receptor homologue with a high threshold for noxious heat, Nature 398 (1999) 436–441.

[9] R. Chokshi, P. Fruasaha, J.A. Kozak, 2-aminoethyl diphenyl borinate (2-APB) inhibits TRPM7 channels through an intracellular acidification mechanism, Channels (Austin) 6 (2012) 362–369.

[10] D.E. Clapham, D. Julius, C. Montell, G. Schultz, International Union of Pharmacology. XLIX. Nomenclature and structure-function relationships of transient receptor potential channels, Pharmacol. Rev. 57 (2005) 427–450.

[11] B. Coste, J. Mathur, M. Schmidt, T.J. Earley, S. Ranade, M.J. Petrus, A.E. Dubin, A. Patapoutian, Piezo1 and Piezo2 are essential components of distinct mechanically activated cation channels, Science 330 (2010) 55–60.

[12] X. Dai, A. Ramji, Y. Liu, Q. Li, E. Karpinski, X. Chen, Inhibition of TRPP3 channel by amiloride and analogs, Mol. Pharmacol. 72 (2007) 1576–1585.

[13] W. Everaerts, B. Nilius, G. Owsianik, The vanilloid transient receptor potential channel TRPV4: from structure to disease, Prog. Biophys. Mol. Biol. 103 (2010) 2–17.

[14] S. Fabris, K. Todoerti, L. Mosca, L. Agnelli, D. Intini, M. Lionetti, S. Guerneri, G. Lambertenghi-Deliliers, F. Bertoni, A. Neri, Molecular and transcriptional characterization of the novel 17p11.2-p12 amplicon in multiple myeloma, Genes Chromosomes Cancer 46 (2007) 1109–1118.

[15] S. Feske, E.Y. Skolnik, M. Prakriya, Ion channels and transporters in lymphocyte function and immunity, Nat. Rev. Immunol. 12 (2012) 532–547.

[16] G. Fois, O. Wittekindt, X. Zheng, E.T. Felder, P. Miklavc, M. Frick, P. Dietl, E. Felder, An ultra fast detection method reveals strain-induced Ca^{2+} entry via TRPV2 in alveolar type II cells, Biomech. Model. Mechanobiol. 11 (2012) 959–971.

[17] P.A. Gottlieb, F. Sachs, Piezo1: properties of a cation selective mechanical channel, Channels 6 (2012) 214–219.

[18] A. Gwanyanya, B. Amuzescu, S.I. Zakharov, R. Macianskiene, K.R. Sipido, V.M. Bolotina, J. Vereecke, K. Mubagwa, Magnesium-inhibited, TRPM6/7-like channel in cardiac myocytes: permeation of divalent cations and pH-mediated regulation, J. Physiol. 559 (2004) 761–776.

[19] C. Harteneck, M. Gollasch, Pharmacological modulation of diacylglycerol-sensitive TRPC3/6/7 channels, Curr. Pharm. Biotechnol. 12 (2011) 35–41.

[20] C. Harteneck, H. Frenzel, R. Kraft, N-(p-amylcinnamoyl)anthranilic acid (ACA): a phospholipase A_2 inhibitor and TRP channel blocker, Cardiovasc Drug Rev. 25 (2007) 61–75.

[21] C. Harteneck, C. Klose, D. Krautwurst, Synthetic modulators of TRP channel activity, in: S. Islam (Ed.), Transient Receptor Potential Channels, Springer, 2011, pp. 87–106.

[22] E.S. Haswell, R. Phillips, D.C. Rees, Mechanosensitive channels: what can they do and how do they do it? Structure 19 (2011) 1356–1369.

[23] E. Hisanaga, M. Nagasawa, K. Ueki, R.N. Kulkarni, M. Mori, I. Kojima, Regulation of calcium-permeable TRPV2 channel by insulin in pancreatic beta-cells, Diabetes 58 (2009) 174–184.

[24] T.C. Ho, N.A. Horn, T. Huynh, L. Kelava, J.B. Lansman, Evidence TRPV4 contributes to mechanosensitive ion channels in mouse skeletal muscle fibers, Channels 6 (2012) 246–254.

[25] H.Z. Hu, Q. Gu, C. Wang, C.K. Colton, J. Tang, M. Kinoshita-Kawada, L.Y. Lee, J.D. Wood, M.X. Zhu, 2-Aminoethoxydiphenyl borate is a common activator of TRPV1, TRPV2, and TRPV3, J. Biol. Chem. 279 (2004) 35741–35748.

[26] R. Inoue, T. Okada, H. Onoue, Y. Hara, S. Shimizu, S. Naitoh, Y. Ito, Y. Mori, The transient receptor potential protein homologue TRP6 is the essential component of vascular α_1-adrenoceptor-activated Ca^{2+}-permeable cation channel, Circ. Res. 88 (2001) 325–332.

[27] A.A. Izzo, F. Borrelli, R. Capasso, V. Di Marzo, R. Mechoulam, Non-psychotropic plant cannabinoids: new therapeutic opportunities from an ancient herb, Trends Pharmacol. Sci. 30 (2009) 515–527.

[28] V. Juvin, A. Penna, J. Chemin, Y.L. Lin, F.A. Rassendren, Pharmacological characterization and molecular determinants of the activation of transient receptor potential V2 channel orthologs by 2-aminoethoxydiphenyl borate, Mol. Pharmacol. 72 (2007) 1258–1268.

[29] R. Kakkar, H. Hei, S. Dobner, R.T. Lee, Interleukin 33 as a mechanically responsive cytokine secreted by living cells, J. Biol. Chem. 287 (2012) 6941–6948.

[30] M. Kanzaki, Y.Q. Zhang, H. Mashima, L. Li, H. Shibata, I. Kojima, Translocation of a calcium-permeable cation channel induced by insulin-like growth factor-1, Nat. Cell Biol. 1 (1999) 165–170.

[31] BJm Kim, K.J. Park, H.W. Kim, S. Choi, J.Y. Jun, I.Y. Chang, J. Jeon, I. So, S.J. Kim, Identification of TRPM7 channels in human intestinal interstitial cells of Cajal, World J. Gastroenterol. 15 (2009) 5799–5804.

[32] R. Kraft, C. Grimm, H. Frenzel, C. Harteneck, Inhibition of TRPM2 cation channels by N-(p-amylcinnamoyl)anthranilic acid, Br. J. Pharmacol. 148 (2006) 264–273.

[33] J.W. Lane, D.W. McBride Jr., O.P. Hamill, Amiloride block of the mechanosensitive cation channel in *Xenopus* oocytes, J. Physiol. 441 (1991) 347–366.

[34] A. Lepple-Wienhues, I. Szabò, T. Laun, N.K. Kaba, E. Gulbins, F. Lang, The tyrosine kinase p56lck mediates activation of swelling-induced chloride channels in lymphocytes, J. Cell Biol. 141 (1998) 281–286.

[35] A. Leffler, R.M. Linte, C. Nau, P. Reeh, A. Babes, A high-threshold heat-activated channel in cultured rat dorsal root ganglion neurons resembles TRPV2 and is blocked by gadolinium, Eur. J. Neurosci. 26 (2007) 12–22.

[36] R.S. Lewis, P.E. Ross, M.D. Cahalan, Chloride channels activated by osmotic stress in T lymphocytes, J. Gen. Physiol. 101 (1993) 801–826.

[37] G. Liu, C. Xie, F. Sun, X. Xu, Y. Yang, T. Zhang, Y. Deng, D. Wang, Z. Huang, L. Yang, S. Huang, Q. Wang, G. Liu, D. Zhong, X. Miao, Clinical significance of transient receptor potential vanilloid 2 expression in human hepatocellular carcinoma, Cancer Genet. Cytogenet. 197 (2010) 54–59.

[38] T.M. Link, U. Park, B.M. Vonakis, D.M. Raben, M.J. Soloski, M.J. Caterina, TRPV2 plays a pivotal role in macrophage particle binding and phagocytosis, Nat. Immunol. 11 (2010) 232–239.

[39] B. Martinac, The ion channels to cytoskeleton connection as potential mechanism of mechanosensitivity, Biochim. Biophys. Acta 1838 (2014) 682–691.

[40] M. Monet, V. Lehen'kyi, F. Gackiere, V. Firlej, M. Vandenberghe, M. Roudbaraki, D. Gkika, A. Pourtier, G. Bidaux, C. Slomianny, P. Delcourt, F. Rassendren, J.P. Bergerat, J. Ceraline, F. Cabon, S. Humez, N. Prevarskaya, Role of cationic channel TRPV2 in promoting prostate cancer migration and progression to androgen resistance, Cancer Res. 70 (2010) 1225–1235.

[41] M.K. Monteilh-Zoller, M.C. Hermosura, M.J. Nadler, A.M. Scharenberg, R. Penner, A. Fleig, TRPM7 provides an ion channel mechanism for cellular entry of trace metal ions, J. Gen. Physiol. 121 (2003) 49–60.

[42] M.B. Morelli, S. Liberati, C. Amantini, M. Nabissi, M. Santoni, V. Farfariello, G. Santoni, Expression and function of the transient receptor potential ion channel family in the hematologic malignancies, Curr. Mol. Pharmacol. 6 (2013) 137–148.

[43] K. Muraki, Y. Iwata, Y. Katanosaka, T. Ito, S. Ohya, M. Shikegawas, Y. Imaizumi, TRPV2 as a component of somatically sensitive cation chanels in murine aortic myocytes, Circ. Res. 93 (2003) 829–838.

[44] M. Nabissi, M.B. Morelli, C. Amantini, V. Farfariello, L. Ricci-Vitiani, S. Caprodossi, A. Arcella, M. Santoni, F. Giangaspero, R. De Maria, G. Santoni, TRPV2 channel negatively controls glioma cell proliferation and resistance to Fas-induced apoptosis in ERK-dependent manner, Carcinogenesis 31 (2010) 794–803.

[45] M. Nabissi, M.B. Morelli, M. Santoni, G. Santoni, Triggering of the TRPV2 channel by cannabidiol sensitizes glioblastoma cells to cytotoxic chemotherapeutic agents, Carcinogenesis 34 (2013) 48–57.

[46] K. Nagata, A. Duggan, G. Kumar, J. Garcia-Anoveros, Nociceptor and hair cell transducer properties of TRPA1, a channel for pain and hearing, J. Neurosci. 25 (2005) 4052–4061.

[47] M.P. Neeper, Y. Liu, T.L. Hutchinson, Y. Wang, C.M. Flores, N. Qin, Activation properties of heterologously expressed mammalian TRPV2. Evidence for species dependence, J. Biol. Chem. 282 (2007) 15894–15902.

[48] B. Nilius, E. Honoré, Sensing pressure with ion channels, Trends Neurosci. 35 (2012) 477–486.

[49] B. Nilius, J. Vriens, J. Prenen, G. Droogmans, T. Voets, TRPV4 calcium entry channel: a paradigm for gating diversity, Am. J. Physiol. Cell Physiol. 286 (2004) C195–C205.

[50] B. Pang, D.H. Shin, K.S. Park, Y.J. Huh, J. Woo, Y. Zhang, T.M. Kang, K. Li, J. Kim, Differential pathways for calcium influx activated by concanavalin A and CD3 stimulation in Jurkat T cells, Pflugers Arch. - Eur. J. Physiol. 463 (2012) 309–318.

[51] M. Parnas, M. Peters, B. Minke, Biophysics of TRP channels, in: E.E. Egelman Channels (Ed.), Comprehensive Biophysics, vol. 6, Elsevier B.V., 2012, pp. 68–107.

[52] N. Qin, M.P. Neeper, Y. Liu, et al., TRPV2 is activated by cannabidiol and mediates CGRP release in cultured rat dorsal root ganglion neurons, J. Neurosci. 28 (2008) 6231–6238.

[53] P.E. Ross, M.D. Cahalan, Ca^{2+} influx pathways mediated by swelling or stores depletion in mouse thymocytes, J. Gen. Physiol. 106 (1995) 415–444.

[54] F. Sachs, Stretch-activated ion channels: what are they? Physiology (Bethesda) 25 (2010) 50–56.

[55] M. Saito, P.I. Hanson, P. Schlesinger, Luminal chloride-dependent activation of endosome calcium channels: patch clamp study of enlarged endosomes, J. Biol. Chem. 282 (2007) 27327–27333.

[56] G. Santoni, V. Farfariello, S. Liberati, M.B. Morelli, M. Nabissi, M. Santoni, C. Amantini, The role of transient receptor potential vanilloid type-2 ion channels in innate and adaptive immune responses, Front. Immunol. 4 (2013) 34.

[57] K. Sauer, T.J. Jegla (2006) Methods for Identifying T Cell Activation Modulating Compounds. Patent ApplicationWO/2006/065613.

[58] T.D. Schmittgen, K.J. Livak, Analyzing real-time PCR data by the comparative C_T method, Nat. Protoc. 3 (2008) 1101–1108.

[59] K. Shibasaki, N. Murayama, K. Ono, Y. Ishizaki, M. Tominaga, TRPV2 enhances axon outgrowth through its activation by membrane stretch in developing sensory and motor neurons, J. Neurosci. 30 (2010) 4601–4612.

[60] G. Spinsanti, R. Zannoli, C. Panti, I. Ceccarelli, L. Marsili, V. Bachiocco, F. Frati, A.M. Aloisi, Quantitative Real-Time PCR detection of TRPV1–4 gene expression in human leukocytes from healthy and hyposensitive subjects, Mol. Pain 4 (2008) 51.

[61] A.V. Staruschenko, E.A. Vedernikova, Mechanosensitive cation channels in human leukaemia cells: calcium permeation and blocking effect, J. Physiol. 541 (2002) 81–90.
[62] A.I. Su, T. Wiltshire, S. Batalov, H. Lapp, K.A. Ching, D. Block, J. Zhang, R. Soden, M. Hayakawa, G. Kreiman, M.P. Cooke, J.R. Walker, J.B. Hogenesch, A gene atlas of the mouse and human protein-encoding transcriptomes, Proc. Natl. Acad. Sci. U. S. A. 101 (2004) 6062–6067.
[63] V. Sydorenko, Y. Shuba, S. Thebault, M. Roudbaraki, G. Lepage, N. Prevarskaya, R. Skryma, Receptor-coupled, DAG-gated Ca^{2+}-permeable cationic channels in LNCaP human prostate cancer epithelial cells, J. Physiol. 548 (2003) 823–836.
[64] C.S. Tremblay, B.J. Curtis, The clonal evolution of leukemic stem cells in T-cell actue lymphoblastic leukemia, Curr. Opin. Hematol. 21 (2014) 320–325.
[65] J. Vriens, G. Appendino, B. Nilius, Pharmacology of vanilloid transient receptor potential cation channels, Mol. Pharmacol. 75 (2009) 1262–1279.
[66] H. Watanabe, J. Vriens, S.H. Suh, C.D. Benham, G. Droogmans, B. Nilius, Heat-evoked activation of TRPV4 channels in a HEK293 cell expression system and in native mouse aorta endothelial cells, J. Biol. Chem. 277 (2002) 47044–47051.
[67] A.S. Wenning, K. Neblung, B. Strauss, M.J. Wolfs, A. Sappok, M. Hoth, E.C. Schwarz, TRP expression pattern and the functional importance of TRPC3 in primary human T-cells, Biochim. Biophys. Acta 1813 (2011) 412–423.
[68] L.J. Wu, T.B. Sweet, D.E. Clapham, International Union of Basic and Clinical Pharmacology. LXXVI. Current progress in the mammalian TRP ion channel family, Pharmacol. Rev. 62 (2010) 381–404.
[69] R. Xia, Z. Mei, H. Mao, W. Yang, L. Dong, H. Bradley, D.J. Beech, L. Jiang, Identification of pore residues engaged in determining divalent cationic permeation in transient receptor potential melastatin subtype channel 2, J. Biol. Chem. 283 (2008) 27426–27432.
[70] S. Xu, F. Zeng, G. Boulay, C. Grimm, C. Harteneck, D.J. Beech, Block of TRPC5 channels by 2-aminoethoxydiphenyl borate: a differential, extracellular and voltage-dependent effect, Br. J. Pharmacol. 145 (2005) 405–414.
[71] T. Yamada, T. Ueda, Y. Shibata, Y. Ikegami, M. Saito, Y. Ishida, S. Ugawa, K. Kohri, S. Shimada, TRPV2 activation induces apoptotic cell death in human T24 bladder cancer cells: a potential therapeutic target for bladder cancer, Urology 76 (509) (2010) e1–e7.
[72] O.V. Yarishkin, E.M. Hwang, J.Y. Park, D. Kang, J. Han, S.G. Hong, Endogenous TRPM4-like channel in Chinese hamster ovary (CHO) cells, Biochem. Biophys. Res. Commun. 369 (2008) 712–717.
[73] T.K. Zagranichnaya, X. Wu, M.L. Villereal, Endogenous TRPC1, TRPC3, and TRPC7 proteins combine to form native store-operated channels in HEK-293 cells, J. Biol. Chem. 280 (2005) 29559–29569.
[74] D. Zhang, A. Spielmann, L. Wang, G. Ding, F. Huang, Q. Gu, W. Schwarz, Mast-cell degranulation induced by physical stimuli involves the activation of transient-receptor-potential channel TRPV2, Physiol. Res. 61 (2012) 113–124.
[75] C. Zitt, A.G. Obukhov, C. Strübing, A. Zobel, F. Kalkbrenner, A. Lückhoff, G. Schultz, Expression of TRPC3 in Chinese hamster ovary cells results in calcium-activated cation currents not related to store depletion, J. Cell Biol. 138 (1997) 1333–1341.